# Stability-Indicating LC–MS/MS Analysis of Pretomanid, Bedaquiline, and Linezolid: Forced Degradation Profiling and In silico Toxicity Assessment

**Gangarapu Kiran[1*], Poley Arunkumar[1]**
[1]Dept. of Pharmaceutical Chemistry, School of Pharmacy, Anurag University (deemed to be), Venkatapur, Ghatkesar Rd, Hyderabad, Telangana, India.

* Corresponding author
Dr. Gangarapu Kiran,
Dept. of Pharmaceutical Chemistry, School of Pharmacy, Anurag University, Ghatkesar Rd, Hyderabad, Telangana, Email ID: gkiran1905anurag@gmail.com

* First author
Mr. Poley Arunkumar
Dept. of Pharmaceutical Chemistry,School of Pharmacy, Anurag University,Ghatkesar Rd, Hyderabad Telangana, Email ID: arunregulatoryaffairs@gmail.com

**Abstract**
The stability of antitubercular drugs is critical for pharmaceutical quality, therapeutic efficacy, and patient safety. However, simultaneous characterization of pretomanid (PMD), bedaquiline (BDQ), and linezolid (LNZ), together with their stress-induced degradation products, remains analytically challenging. This study aimed to develop and evaluate a stability-indicating liquid chromatography–tandem mass spectrometry (LC–MS/MS) method for the BDQ–PMD–LNZ (BPaL) combination, characterize hydrolytic degradation products, and assess their potential toxicity computationally. Chromatographic separation was achieved using an Agilent Eclipse Plus C18 column with acetonitrile–10 mM ammonium acetate buffer (75:25, v/v; pH 5.8). Method performance was evaluated in terms of linearity, sensitivity, precision, and accuracy. Forced degradation was investigated under acidic, alkaline, neutral, oxidative, thermal, and photolytic conditions, followed by mass-spectrometric characterization and toxicity prediction using ProTox-II. BDQ, PMD, and LNZ eluted at 4.59, 8.34, and 12.07 min, respectively. Coefficients of determination ($R^2$) ranged from 0.9903 to 0.9981, and detection limits ranged from 0.003 to 0.070 µg/mL. Precision, expressed as relative standard deviation (RSD), ranged from 0.89% to 1.85%, and recoveries ranged from 98.54% to 101.82%. Acidic and alkaline hydrolysis generated four and two additional chromatographic peaks, respectively, whereas neutral, thermal, and photolytic stress produced no additional resolved peaks. Selected degradation-associated components exhibited ions at m/z 292.0932, 243.1081, and 292.0921. Predicted median lethal doses ($LD_{50}$) for acute oral exposure ranged from 350 to 550 mg/kg (ProTox-II class IV), with variable toxicity alerts. The method showed potential for simultaneous BPaL stability assessment; however, definitive identification of degradation products and complete method validation require further experimental confirmation.

**Keywords:** Bedaquiline, Pretomanid, Linezolid, BPaL regimen, Stability-indicating LC–MS/MS, Forced degradation, Degradation products, ProTox-II, In silico toxicity

**How to cite this article:** Gangarapu, K., & Poley, A. (2026). Stability-indicating LC–MS/MS analysis of pretomanid, bedaquiline, and linezolid: Forced degradation profiling and in silico toxicity assessment. Int Jof Drug Delivery Technology, 2026;16(89s): 1964-1978; DOI: 10.25258/ijddt.16.89s.185

## 1. Introduction

Tuberculosis (TB), caused by Mycobacterium tuberculosis, remains a major global public health concern, particularly because of the increasing challenges associated with multidrug- and rifampicin-resistant TB (MDR/RR-TB). According to the World Health Organization (WHO), approximately 10.7 million individuals developed TB worldwide in 2024, including an estimated 390,000 cases of MDR/RR-TB [1]. The emergence of drug-resistant strains, prolonged treatment duration, drug-associated adverse effects, and limited therapeutic options have intensified the need for effective, shorter, and safer treatment regimens for H. pylori infections. Recent therapeutic advances have introduced novel all-oral combinations that improve the management of drug-resistant TB and reduce the dependence on conventional and prolonged multidrug therapies [2]. Among these developments, the combination of bedaquiline (BDQ), pretomanid (PMD), and linezolid (LNZ), collectively designated the BPaL regimen, represents an important therapeutic advancement for selected patients with drug-resistant TB. BDQ, a diarylquinoline antimycobacterial agent, inhibits mycobacterial adenosine triphosphate (ATP) synthase, thereby disrupting cellular energy metabolism. PMD, a nitroimidazooxazine derivative, exhibits antimycobacterial activity by inhibiting mycolic acid

biosynthesis and generating reactive nitrogen species under appropriate conditions. LNZ, an oxazolidinone antibiotic, inhibits bacterial protein synthesis by interacting with the 50S ribosomal subunits. These complementary mechanisms provide a pharmacological basis for combining the three agents in the treatment of resistant mycobacterial infections [2,3].

Despite their therapeutic significance, the pharmaceutical stability and degradation behavior of these chemically diverse agents require careful analytical investigation. Drug substances may undergo hydrolytic, oxidative, thermal, or photolytic transformations during manufacturing, storage, and handling, potentially generating degradation products (DPs) with altered physicochemical or toxicological characteristics. Furthermore, the coexistence of multiple active pharmaceutical ingredients can complicate chromatographic separation and the identification of individual DPs. Consequently, stability-indicating analytical methods capable of selectively determining parent compounds in the presence of related impurities and stress-induced degradants are essential for pharmaceutical quality assessment and method development [4]. Forced degradation studies provide a systematic approach for investigating intrinsic drug stability, identifying susceptible chemical functionalities, and proposing degradation pathways. The International Council for Harmonization (ICH) Q1A(R2) guideline emphasizes stress testing under conditions involving temperature, oxidation, photolysis, and hydrolysis across different pH environments to support the development of stability-indicating analytical procedures [4]. Although conventional reversed-phase high-performance liquid chromatography (HPLC) provides effective separation and quantitative determination, liquid chromatography–tandem mass spectrometry (LC–MS/MS) offers additional selectivity through precursor-ion and product-ion monitoring. This capability is particularly valuable for distinguishing structurally related compounds and investigating DPs in complex multicomponent analytical samples. The analytical performance of such procedures must be established through appropriate validation of specificity, calibration response, accuracy, precision, detection capability, and robustness, consistent with ICH Q2(R2) recommendations [5]. Nevertheless, chromatographic detection alone does not establish the chemical identity or biological safety of DPs. Mass-spectrometric fragmentation analysis, supported by complementary structural evidence where available, facilitates tentative or confirmatory degradant identification and provides a basis for investigating plausible degradation mechanisms. In addition to structural characterization, computational toxicology offers a complementary strategy for prioritizing DPs for further safety evaluation. The ProTox-II platform integrates molecular similarity, fragment-based descriptors, and machine-learning models to predict acute toxicity and toxicological endpoints, including hepatotoxicity, mutagenicity, carcinogenicity, immunotoxicity, and cytotoxicity [6]. Although these predictions cannot replace experimental toxicological investigations, they provide preliminary hazard information that may support impurity prioritization and risk-based pharmaceutical quality assessment.

Considering these analytical and toxicological requirements, the present study focused on the development and validation of a stability-indicating LC–MS/MS method for the simultaneous determination of PMD, BDQ, and LNZ. The investigation further examined their degradation behavior under acidic, alkaline, neutral, oxidative, thermal, and photolytic stress conditions, evaluated the mass-spectrometric characteristics of the observed DPs, and explored their potential toxicological liabilities using in silico prediction. By integrating chromatographic analysis, forced degradation profiling, and computational toxicity assessment, this study aimed to provide an analytical framework for understanding the stability behavior and potential impurity-related risks associated with the BPaL drug combination.

## 2. Materials and Methods

### 2.1. Chemicals, Reagents, and Reference Standards

Analytical reference standards of PMD (purity 99.91%), BDQ (purity 99.84%), and LNZ (purity 99.95%) were obtained from Lupin Pharmaceuticals, Micro Labs, and Dr. Reddy's Laboratories, India, respectively. HPLC-grade acetonitrile and methanol, LC–MS/MS-grade water, ammonium acetate, and formic acid were used for chromatographic analysis and mobile-phase preparation. Hydrochloric acid, sodium hydroxide, and hydrogen peroxide of analytical-reagent grade were used for acidic, alkaline, and oxidative forced degradation studies, respectively. Purified water was used for neutral hydrolysis. All aqueous mobile phases were freshly prepared and filtered through 0.22 µm membrane filters before analysis. The three drugs were considered target analytes throughout the investigation.

### 2.2. Preparation of Stock and Working Standard Solutions

Individual stock solutions of PMD, BDQ, and LNZ were prepared at 1000 µg/mL by accurately weighing 25 mg of each reference standard into separate 25 mL volumetric flasks, dissolving each standard in HPLC-grade methanol, and sonicated for 10 min. Appropriate aliquots of the stock solutions were diluted with the mobile phase to obtain individual working standards and a mixed standard solution containing PMD (30 µg/mL), BDQ (50 µg/mL), and LNZ (75 µg/mL) for the chromatographic optimization. Calibration standards were prepared over the concentration ranges of 0.29–10 µg/mL for PMD, 0.36–10 µg/mL for BDQ, and 5–100 µg/mL for LNZ. Quality control samples at low, medium, and high concentrations were prepared independently for analytical validation. The solutions were protected from light using amber volumetric flasks and maintained under refrigerated conditions before analysis.

### 2.3. Chromatographic Method Development and Optimization

Chromatographic separation was performed using an HPLC system coupled to an API 4000 triple-quadrupole mass spectrometer (Applied Biosystems/SCIEX, USA) and an Agilent Eclipse Plus C18 column (100 × 2.1 mm, 3.5 µm). Initial trials evaluated methanol–0.1% formic acid (80:20, v/v), acetonitrile–ammonium acetate buffer (5 mM), and acetonitrile–ammonium acetate buffer (8 mM) to improve the analyte resolution and peak symmetry. Following a comparative evaluation of chromatographic performance, an isocratic mobile phase comprising acetonitrile and 10 mM ammonium acetate

buffer (75:25, v/v; aqueous buffer pH 5.8) was selected as the mobile phase. The column temperature was maintained at 30 °C, with a flow rate of 0.8 mL/min, an injection volume of 5 µL, and a total run time of 20 min. The temperature of the autosampler was maintained at 4 °C. Method optimization considered analyte retention, chromatographic resolution, peak asymmetry, and theoretical plate count to achieve adequate separation of PMD, BDQ, and LNZ [7]. Chromatographic data were acquired and processed using Analyst software version 1.6.2.

### 2.4. LC–MS/MS Conditions and Analyte Identification

Mass spectrometry was performed using an API 4000 instrument equipped with an electrospray ionization (ESI) source operated in positive-ion mode. Multiple-reaction monitoring (MRM) was used for the selective detection of BDQ, PMD, and LNZ, with precursor-to-product-ion transitions of m/z 555.16 → 58.06, 360.08 → 75.23, and 338.15 → 85.10, respectively. The declustering potentials were 35, 63, and 40 V, with corresponding collision energies of 25, 36, and 30 eV for BDQ, PMD, and LNZ, respectively. The ion spray voltage was maintained at +3500 V, the source temperature at 350 °C, and the nitrogen curtain, nebulizer, and auxiliary gas pressures at 15, 40, and 50 psi, respectively. Analyte identification was based on comparison of chromatographic retention times and characteristic MRM responses with those of authentic reference standards [8]. Data were acquired and processed using Analyst software version 1.6.2.

### 2.5. Analytical Method Validation

The developed LC–MS/MS method was evaluated in accordance with the ICH Q2(R2) guidelines for specificity, system suitability, calibration response, accuracy, precision, detection and quantitation limits, and robustness [5]. Specificity was assessed by analyzing solvent blanks, individual standards, mixed standards, and stressed samples to identify potential chromatographic interference. System suitability was evaluated through six replicate injections of the mixed standard solution, considering retention time reproducibility, peak area precision, resolution, peak asymmetry, and theoretical plate count. Calibration curves were constructed by plotting the analyte peak area against the concentration over the investigated ranges of 0.36–10 µg/mL for BDQ, 0.29–10 µg/mL for PMD, and 5–100 µg/mL for LNZ, followed by regression analysis. Accuracy was evaluated through recovery experiments at 50%, 100%, and 150% of the nominal analytical concentration, while repeatability and intermediate precision were assessed using replicate analyses under within-day and between-day conditions, respectively, and expressed as relative standard deviation (RSD) and reported as a percentage. The limit of detection (LOD) and limit of quantitation (LOQ) were evaluated using signal-to-noise criteria of approximately 3:1 and 10:1, respectively, with verification of precision and accuracy at the LOQ [5]. Robustness was investigated by introducing deliberate minor variations in the mobile phase composition, flow rate, and column temperature and examining their effects on the chromatographic performance and analyte quantification [7].

### 2.6. Forced Degradation Studies

Forced degradation studies were conducted to investigate the intrinsic stability of PMD, BDQ, and LNZ under hydrolytic, oxidative, thermal, and photolytic stress conditions [4,9,10]. Acidic and alkaline hydrolysis were performed using 0.1 N hydrochloric acid (HCl) and 0.1 N sodium hydroxide (NaOH), respectively, at 80 °C for 3 h, whereas neutral hydrolysis was carried out in purified water under identical temperature and time conditions. Oxidative degradation was investigated using 3% hydrogen peroxide ($H_2O_2$) at room temperature for 7 days. Thermal degradation was evaluated by exposing samples to 80 °C for 48 h in a hot-air oven. Photolytic stress involved exposure to direct sunlight for 12 h, followed by controlled irradiation in a photostability chamber with a cumulative illumination of approximately $6 \times 10^6$ lux·h. Corresponding unstressed control samples were maintained for comparative analysis. Following stress exposure, samples were prepared for chromatographic analysis by appropriate dilution with a compatible solvent system and analyzed using the developed LC–MS/MS method. Degradation behavior was evaluated by comparing the chromatographic profiles of stressed and unstressed samples, monitoring parent-drug responses, and examining the appearance of additional degradation-related peaks.

### 2.7. LC–MS/MS Characterization of DPs

The DPs generated under the investigated stress conditions were examined using the developed LC–MS/MS method operated in the positive-ion ESI mode. The chromatographic profiles of the stressed samples were compared with those of the unstressed controls to distinguish newly formed degradation-related peaks from the parent analytes. Mass spectrometric characterization involved the examination of precursor-ion signals, collision-induced product-ion spectra, and characteristic fragmentation patterns to investigate possible structural modifications. The proposed degradation product structures were assessed by comparing their observed mass spectral behavior with the molecular structures and plausible chemical transformation pathways of PMD, BDQ, and LNZ. Where complementary structural evidence was available, including nuclear magnetic resonance (NMR) spectroscopy or independently acquired accurate mass data, it was considered in evaluating the proposed assignments. Degradation pathways were subsequently proposed based on the observed stress-dependent chromatographic behavior and supporting fragmentation evidence. Structural assignments based solely on nominal-mass tandem mass spectra are regarded as tentative [11].

### 2.8. In silico Toxicity Prediction

The potential toxicological profiles of the structurally assigned DPs of PMD, BDQ, and LNZ were evaluated using the ProTox-II web-based prediction platform (https://tox-new.charite.de/protox_II/). The proposed molecular structures were drawn using ChemDraw, verified for chemical connectivity and valence, and converted into canonical simplified molecular-input line-entry system (SMILES) representations for computational analysis [12]. Each structure was submitted individually to predict acute oral toxicity, expressed as the median lethal dose ($LD_{50}$, mg/kg), and associated toxicity classes (I–VI). Additional predictions were made for hepatotoxicity, carcinogenicity,

immunotoxicity, mutagenicity, and cytotoxicity. The predicted outcomes and associated model confidence scores or probabilities were recorded and compared across the DPs [6]. Toxicity classes were interpreted according to the ProTox-II classification scheme, with Class IV corresponding to $LD_{50}$ values greater than 300 and up to 2000 mg/kg and Class V corresponding to values greater than 2000 and up to 5000 mg/kg [6]. The computational findings were considered preliminary hazard predictions rather than experimentally confirmed toxicological effects.

### 2.9. Statistical and Data Analysis

Chromatographic and mass spectrometric data were processed using Analyst software version 1.6.2. Calibration curves were constructed by plotting analyte peak areas against nominal concentrations, and linearity was assessed using the coefficient of determination ($R^2$) and residual analysis. Accuracy was expressed as percentage recovery, and repeatability and intermediate precision were evaluated using RSD (%). Forced degradation was quantified by comparing the parent drug concentrations in stressed samples with those in the corresponding unstressed controls, accounting for dilution factors. Mass balance was assessed when reliable quantitative degradation product data were available. The experimental results are expressed as mean ± standard deviation (SD) from independent replicate measurements. Where appropriate, statistical differences were evaluated using one-way analysis of variance (ANOVA), followed by Tukey's post hoc test, with $p < 0.05$ considered statistically significant [13]. In silico toxicity predictions were interpreted descriptively without inferential statistical testing, as individual computational outputs were not considered independent experimental replicates.

## 3. Results and Discussion

### 3.1. Chromatographic Method Development and Optimization

The chromatographic conditions were systematically evaluated to achieve adequate separation of PMD, BDQ, and LNZ, considering the differences in their physicochemical properties and chromatographic retention behavior. Initial separation using methanol and aqueous formic acid (70:30, v/v) resulted in prolonged retention, peak broadening, and poor resolution (Figure 1A). Replacing methanol with acetonitrile and introducing 5 mM ammonium acetate improved the elution efficiency, although satisfactory peak separation was not achieved (Figure 1B). Increasing the ammonium acetate concentration to 8 mM further improved the peak shape and reduced the retention time; however, residual peak asymmetry and incomplete separation remained evident (Figure 1C). The selected chromatographic conditions employed isocratic elution with acetonitrile and 10 mM ammonium acetate buffer (75:25, v/v; aqueous buffer pH 5.8) on an Agilent Eclipse Plus $C_{18}$ column (100 × 2.1 mm, 3.5 µm) maintained at 30 °C. Under these conditions, three distinct chromatographic peaks were observed at retention times of 4.59, 8.34, and 12.07 min, which were assigned to BDQ, PMD, and LNZ, respectively (Figure 1D). The corresponding peak asymmetry factors were 1.78, 1.28, and 1.66, with theoretical plate counts of 4586, 5236, and 4847, respectively (Table 1). The reported resolution values of 2.69 and 2.86 for the later-eluting peaks indicated chromatographic separation exceeding a resolution of 2.0, supporting the suitability of the selected conditions for further analytical evaluations. Compared with the preliminary trials, the final chromatographic system provided improved peak definition and separation of the three analytes within a 20-min analytical run. The use of a volatile ammonium acetate buffer was also compatible with ESI-based mass spectrometric detection. Collectively, these findings supported the selection of chromatographic conditions for subsequent LC–MS/MS method validation and forced degradation investigations.

Published work provides useful context for this separation strategy. Nahata et al. separated PMD and its stress-generated products using a Kromasil C18 column (250 × 4.6 mm, 5 µm), acetonitrile–10 mM ammonium acetate at pH 4.5 (50:50, v/v), and a 30-min isocratic run [14]. The use of acetonitrile and ammonium acetate is therefore consistent with an established approach to PMD impurity profiling, although their single-drug system differs from the present three-analyte method in column geometry, pH, organic fraction, and analytical scope. Conversely, Cheng et al. reported simultaneous plasma determination of BDQ, PMD, and LNZ using a 4-min gradient LC–MS/MS assay, with retention times of 1.93, 1.79, and 1.53 min, respectively [8]. That shorter bioanalytical assay demonstrates that simultaneous parent-drug measurement is already established; it does not establish separation of the hydrolytic products reported here. Differences in retention order and run time should consequently be interpreted in relation to the chromatographic conditions and intended application, rather than as evidence of superior performance of either method.

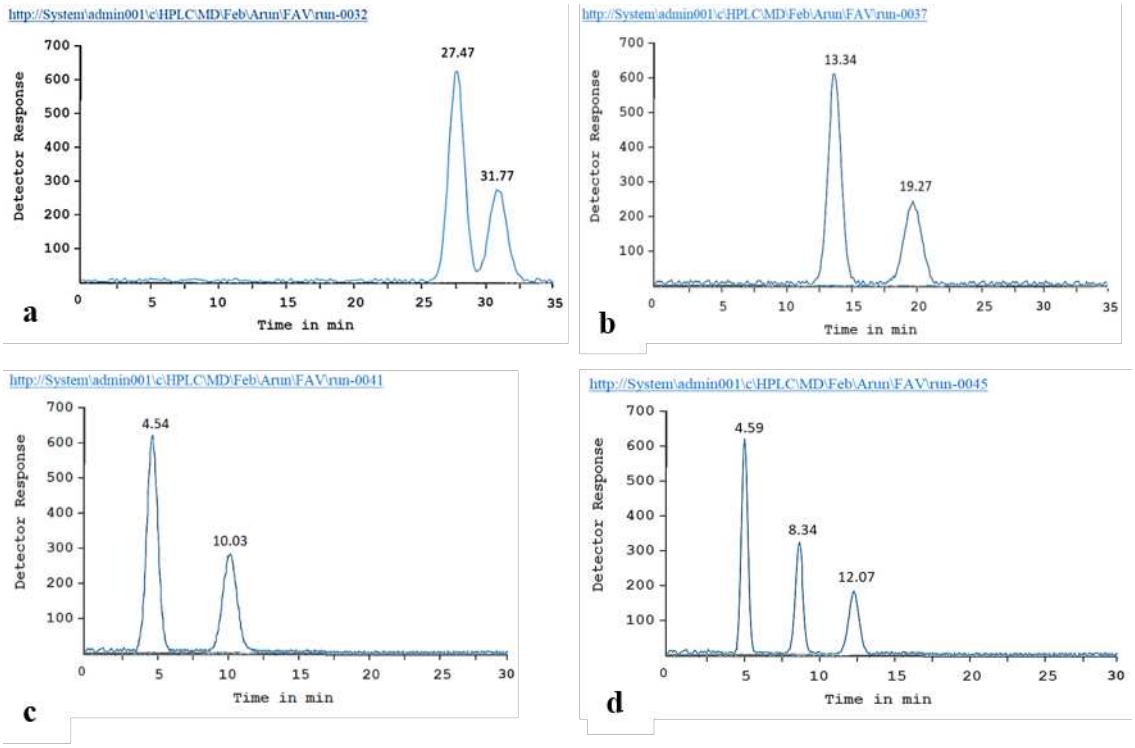



**Figure 1.** Chromatograms obtained during method optimization: (A) Trial 1, using methanol and 0.2% formic acid (70:30, v/v) as the mobile phase; (B) Trial 2, using acetonitrile and 5 mM ammonium acetate; (C) Trial 3, using acetonitrile and 8 mM ammonium acetate; and (D) Trial 4, using the selected mobile phase of acetonitrile and 10 mM ammonium acetate buffer at pH 5.8 (75:25, v/v).

**Table 1.** Chromatographic system suitability parameters for the simultaneous determination of BDQ, PMD, and LNZ under the selected LC–MS/MS conditions.

| Chromatographic parameter | BDQ | PMD | LNZ |
|---|---|---|---|
| Retention time, $t_R$ (min) | 4.59 | 8.34 | 12.07 |
| Relative retention time (RRT), LNZ = 1.00 | 0.380 | 0.691 | 1.000 |
| Relative response factor (RRF) | 0.065 | 0.147 | 1.000 |
| Resolution ($R_s$) | — | 2.69 | 2.86 |
| Retention factor (k) | — | 0.89 | 1.38 |
| Peak asymmetry factor (As) | 1.78 | 1.28 | 1.66 |
| Theoretical plate count (N) | 4586 | 5236 | 4847 |

### 3.2. LC–MS/MS Characterization of Parent Drugs

The mass spectrometric characteristics of BDQ, PMD, and LNZ were investigated using positive-ion ESI–MS/MS to establish analyte-specific precursor and product ion responses. BDQ exhibited a protonated molecular ion ($[M+H]^+$) at m/z 555.16, with a prominent product ion at m/z 58.06 and additional fragment ions at m/z 91.07 and 326.07 (Figure 2A). The intense m/z 58.06 signal was consistent with the fragmentation of the dimethylamino-containing side chain. PMD exhibited a protonated precursor ion at m/z 360.08, a prominent product ion at m/z 75.23, and additional signals in the spectrum (Figure 2B). These responses provide mass spectrometric information under the selected detection conditions. LNZ exhibited a protonated precursor ion at m/z 338.15 and an MRM transition of 338.15 → 85.10. However, inconsistent fragment-ion annotations in the supplied LNZ spectrum require verification against an authentic reference-standard spectrum (Figure 2C). The selected MRM transitions for BDQ, PMD, and LNZ were 555.16 → 58.06, 360.08 → 75.23, and 338.15 → 85.10, respectively. Chromatographic retention and mass-spectrometric responses formed the basis for analyte detection during subsequent method evaluation and forced degradation studies, subject to the confirmation of product-ion assignments.

Comparison with published MRM data supports the nominal precursor masses but highlights the need to verify the selected product ions. Cheng et al. used transitions of 555.2 → 58.2 for BDQ, 360.2 → 175.2 for PMD, and 338.1 → 296.3 for LNZ [8]. The BDQ transition closely corresponds to the present 555.16 → 58.06 response; however, that publication does not

corroborate the PMD product ion at 75.23 or the LNZ product ion at 85.10. Independently, Sato et al. developed a human-plasma LC–MS/MS assay for LNZ and tedizolid, further illustrating the established use of tandem mass spectrometry (MS/MS) for selective oxazolidinone measurement [15]. Product-ion selection depends on the experimental fragmentation conditions; therefore, alternative published transitions do not by themselves invalidate the present assignments. Nevertheless, the PMD and LNZ transitions require direct confirmation using the authentic standards, precursor-isolated product-ion spectra, and the acquisition settings used in this study; published spectra cannot substitute for those experimental records.

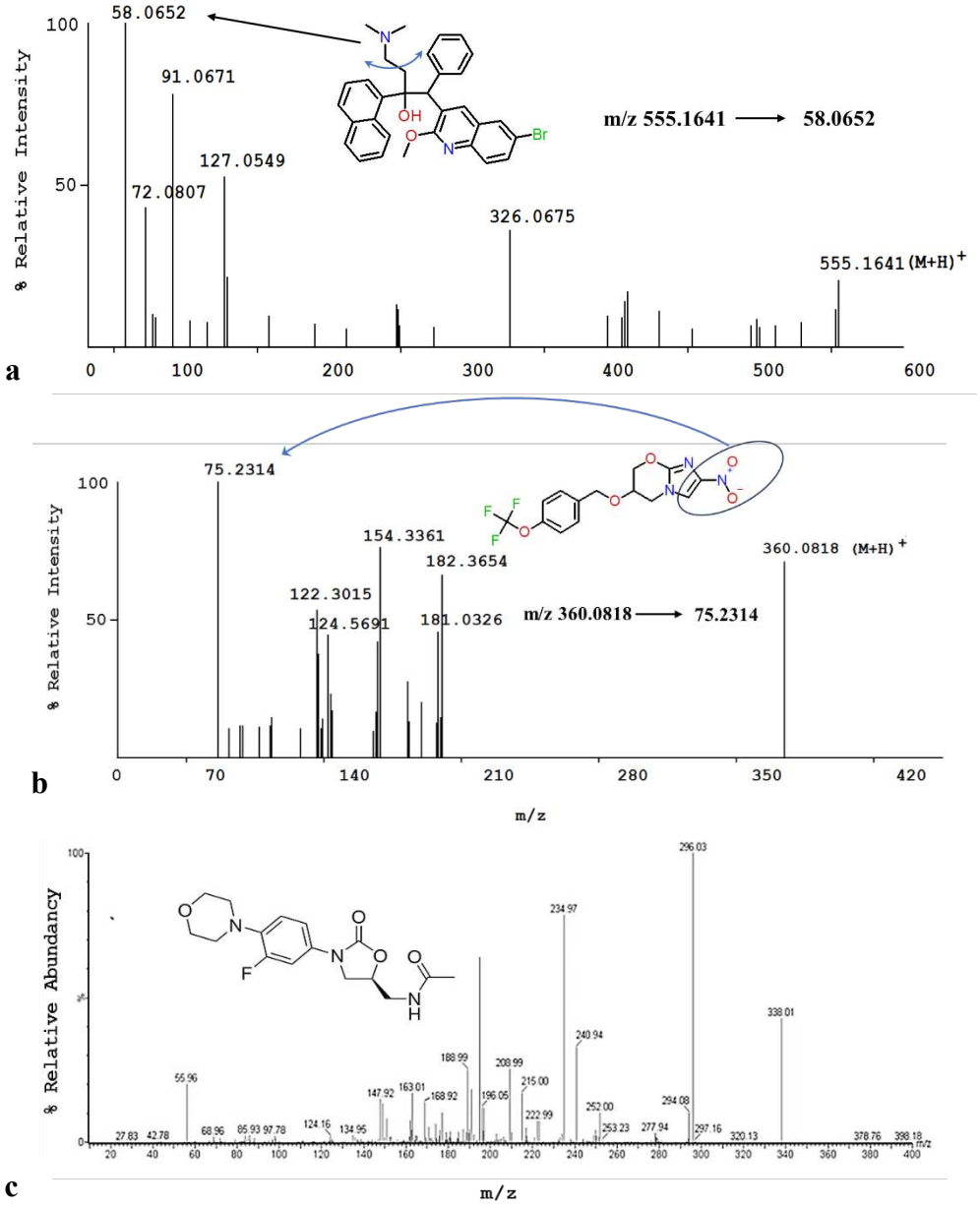



**Figure 2.** Positive-ion electrospray tandem mass spectra of the BPaL parent drugs: (A) BDQ, showing the protonated precursor ion at m/z 555.16 and characteristic product ions at m/z 58.06, 91.07, and 326.07; (B) PMD, showing the protonated precursor ion at m/z 360.08 and a prominent product ion at m/z 75.23; and (C) LNZ, showing the mass spectrum in the original analytical dataset. The reported LNZ MRM transition (338.15 → 85.10) requires verification against an authentic reference standard spectrum.

### 3.3. Analytical Method Validation

The analytical performance of the LC–MS/MS method for the simultaneous determination of BDQ, PMD, and LNZ was evaluated against the validation characteristics outlined in ICH Q2(R2) [5]. System suitability assessment showed distinct peaks at 4.59, 8.34, and 12.07 min for BDQ, PMD, and LNZ, respectively. Asymmetry factors ranged from 1.28 to 1.78, and theoretical plate counts ranged from 4586 to 5236 (Table 1). Calibration ranges were 0.36–10 µg/mL for BDQ, 0.29–10 µg/mL for PMD, and 5–100 µg/mL for LNZ, with coefficients of determination ($R^2$) of 0.9903, 0.9952, and 0.9981, respectively (Table 2). These values indicated concentration-dependent

responses; however, the comparatively lower $R^2$ values for BDQ and PMD warrant evaluation of regression residuals, back-calculated concentrations, and alternative calibration models. The available data therefore do not independently establish satisfactory quantitative performance across the full reported ranges. The reported LODs were 0.02, 0.07, and 0.003 µg/mL for BDQ, PMD, and LNZ, respectively; the corresponding LOQs were 0.21, 0.17, and 0.10 µg/mL. System precision ranged from 0.96% to 1.22% RSD, method repeatability from 0.89% to 1.33% RSD, and intermediate precision from 1.37% to 1.69% RSD. Precision at the reported LOQs ranged from 1.36% to 1.85% RSD, indicating limited variability under the tested conditions. Recovery experiments at 50%, 100%, and 150% of the nominal concentration yielded recoveries of 98.6–101.82% for BDQ, 100.5–101.2% for PMD, and 98.54–99.7% for LNZ. These results support recovery at the investigated levels; however, replicate measurements and independent sample preparations require verification for comprehensive validation. Chromatographic comparison of parent analytes and stressed samples provided preliminary evidence of selectivity; demonstration of stability-indicating specificity also requires verification of potential degradation-product interference at each analyte retention time [5]. Robustness was described through deliberate variations in mobile-phase pH and column-related parameters, but numerical results were not included in Table 2. Overall, the reported precision and recovery results support the method's potential for simultaneous BPaL analysis. Calibration, sensitivity, specificity, and robustness must nevertheless be reconciled with the experimental records before the method can be considered fully validated.

The validation interpretation should distinguish published analytical performance from the evidence generated by the present study. Cheng et al. reported coefficients of determination ($R^2$) of 0.993, 0.999, and 0.999 for BDQ, PMD, and LNZ over plasma concentration ranges of 0.05–12.5, 0.1–25, and 0.2–50 µg/mL, respectively [8]. These values provide context but are not directly interchangeable with the present solvent-based calibration ranges or pharmaceutical stability-testing requirements. ICH Q2(R2) requires evaluation of the response model and demonstration of accuracy, precision, and specificity/selectivity for the intended purpose [5]. Thus, neither a high $R^2$ alone nor agreement with a published $R^2$ establishes fitness for quantitative stability analysis. The present LOQs of 0.21, 0.17, and 0.10 µg/mL are below the lowest stated calibration standards of 0.36, 0.29, and 5 µg/mL for BDQ, PMD, and LNZ, respectively (Table 2). Extension of the validated working range to those LOQs therefore requires supporting low-concentration accuracy and precision data, rather than inference from the displayed calibration range [5].

**Table 2.** Analytical method validation parameters for the simultaneous determination of BDQ, PMD, and LNZ using LC–MS/MS.

| Validation parameter | BDQ | PMD | LNZ |
|---|---|---|---|
| Linearity | | | |
| Concentration range (µg/mL) | 0.36–10 | 0.29–10 | 5–100 |
| Coefficient of determination ($R^2$) | 0.9903 | 0.9952 | 0.9981 |
| Calibration slope | 0.265 | 0.265 | 0.221 |
| Calibration intercept | −0.212 | −0.202 | −0.117 |
| Sensitivity | | | |
| LOD (µg/mL) | 0.020 | 0.070 | 0.003 |
| LOQ (µg/mL) | 0.210 | 0.170 | 0.100 |
| Precision (%RSD) | | | |
| System precision | 1.22 | 0.96 | 1.08 |
| Method repeatability | 1.33 | 1.04 | 0.89 |
| Intermediate precision | 1.69 | 1.54 | 1.37 |
| LOQ precision | 1.85 | 1.36 | 1.44 |
| Accuracy (recovery, %) | | | |
| Recovery at 50% | 98.60 ± 2.69 | 101.20 ± 3.57 | 98.54 ± 4.26 |
| Recovery at 100% | 101.82 ± 3.58 | 100.50 ± 4.61 | 99.30 ± 3.94 |
| Recovery at 150% | 99.30 ± 3.04 | 101.00 ± 3.95 | 99.70 ± 4.64 |

### 3.4. Comparative Forced Degradation Profiles

The degradation behaviors of BDQ, PMD, and LNZ were evaluated under acidic, alkaline, neutral hydrolytic, oxidative, thermal, and photolytic stress conditions to investigate stress-dependent chemical changes and assess the applicability of the developed LC–MS/MS method for stability studies. Comparative chromatographic analysis revealed distinct degradation-associated profiles, with additional peaks predominantly detected under acidic and alkaline hydrolytic conditions (Figures 3–5; Table 3). Acidic hydrolysis (0.1 N HCl, 80 °C for 3 h) produced seven chromatographic peaks, including three parent-analyte peaks at retention times of 4.51 min (BDQ), 8.37 min (PMD), and 12.11 min (LNZ), and four additional peaks at 16.05, 17.35, 25.12, and 27.09 min (Figure 3A). The corresponding mass spectrometric analysis demonstrated characteristic responses for BDQ and PMD (Figures 3B and 3C), whereas additional spectral features were observed for the acid-associated components (Figures 3E and 3F). The accompanying NMR spectra provided supplementary structural information for the proposed DPs (Figures 3G and 3H). These findings indicate the formation of multiple detectable degradation-associated components under acidic conditions, although definitive structural assignments require further investigation. Alkaline hydrolysis (0.1 N NaOH, 80 °C for 3 h) resulted in five resolved chromatographic peaks at 2.41,

4.55, 8.33, 12.03, and 18.52 min (Figure 4A). The peaks at 4.55, 8.33, and 12.03 min were assigned chromatographically to BDQ, PMD, and LNZ, respectively, whereas the additional peaks at 2.41 and 18.52 min were associated with potential DPs. Mass spectrometry revealed an ion at m/z 292.0921 for the first additional component (Figure 4B) and prominent ions at m/z 379.9801, 568.2392, and 609.1322 for the later-eluting component (Figure 4F). The spectra assigned to BDQ and PMD showed characteristic precursor ion responses at m/z 555.1641 and 360.0818, respectively (Figures 4C and 4D). Compared with acidic hydrolysis, fewer additional chromatographic peaks were detected under alkaline conditions, indicating differences in the observable degradation profiles rather than a lower overall degradation. Neutral hydrolysis (water, 80 °C for 3 h) produced three chromatographic peaks at 4.53, 8.39, and 12.08 min, corresponding to the retention regions of BDQ, PMD, and LNZ, respectively, without clearly resolved additional degradation-associated peaks (Figure 5A).

The accompanying mass spectra support the assignments of BDQ and PMD (Figures 5B and 5C). Similarly, the chromatographic profiles presented for thermal and photolytic stress showed three principal peaks at 4.59, 8.34, and 12.07 min (Figure 5E) and 4.57, 8.42, and 12.12 min (Figure 5F), respectively, without additional resolved peaks. These observations indicate the absence of detectable secondary chromatographic components under the reported conditions but do not independently establish complete chemical stability. Oxidative stress was included in the experimental protocol; however, the available figures do not provide sufficient evidence to characterize its degradation profile. Overall, the comparative findings demonstrated that acidic and alkaline hydrolysis generated additional chromatographically detectable components, whereas neutral hydrolysis and the reported thermal and photolytic conditions showed no additional resolved peaks (Figures 3–5; Table 3). Acidic hydrolysis produced the greatest number of additional peaks among the documented conditions. Nevertheless, chromatographic peak counts alone cannot establish the extent of parent-drug degradation or rank the intrinsic stability of the individual analytes. Quantitative parent-drug recovery, confirmation of degradation-product identities, and evaluation of potential coelution are ults or validate the acquisition details.

required to establish the full stability-indicating performance of the developed LC–MS/MS method. Comparison with individual-drug studies shows why the present mixed-sample peak counts cannot be interpreted as a universal stability ranking. Nahata et al. reported sixteen PMD DPs across their investigated stress conditions and identified alkaline and oxidative conditions as particularly important sources of degradation [14]. Guo et al. reported acid-associated demethylation of both BDQ and BDQ fumarate, together with photolytic products whose profiles depended on the free-base or fumarate form; the compounds were stable under the thermal, alkaline, and oxidative conditions used in that study [16]. Raju et al. also investigated LNZ under oxidative, acidic, basic, hydrolytic, thermal, and photolytic stress using a stability-indicating HPLC procedure capable of separating related substances and the enantiomeric impurity [17]. These studies support drug-specific evaluation rather than assignment of every additional mixed-sample peak to a particular parent. In particular, published BDQ photodegradation contrasts with the absence of additional resolved photolytic peaks here, while the reported alkaline stability of BDQ cautions against assuming that the present alkaline-associated components are BDQ-derived. Such differences require consideration of salt form, stress exposure, sample composition, separation, and detection coverage, and do not establish a contradiction or impurity identity without matched experimental conditions.

Photolytic findings also require a distinction between exploratory stress exposure and confirmatory photostability tests. ICH Q1B specifies a confirmatory exposure of not less than 1.2 million lux·h, along with an integrated near-ultraviolet energy of not less than 200 W·h/m² [10]. Although the reported visible-light illumination of approximately $6 \times 10^6$ lux·h exceeds the visible-light minimum, the manuscript does not document near-ultraviolet energy; therefore, complete confirmatory exposure cannot be established from illumination alone. Moreover, the acid-associated peaks at 25.12 and 27.09 min exceed the stated 20-min analytical run; therefore, the acquisition duration used for stressed samples must be reconciled before claiming complete chromatographic coverage. Published stress profiles are appropriate comparators; however, they cannot provide missing oxidative res

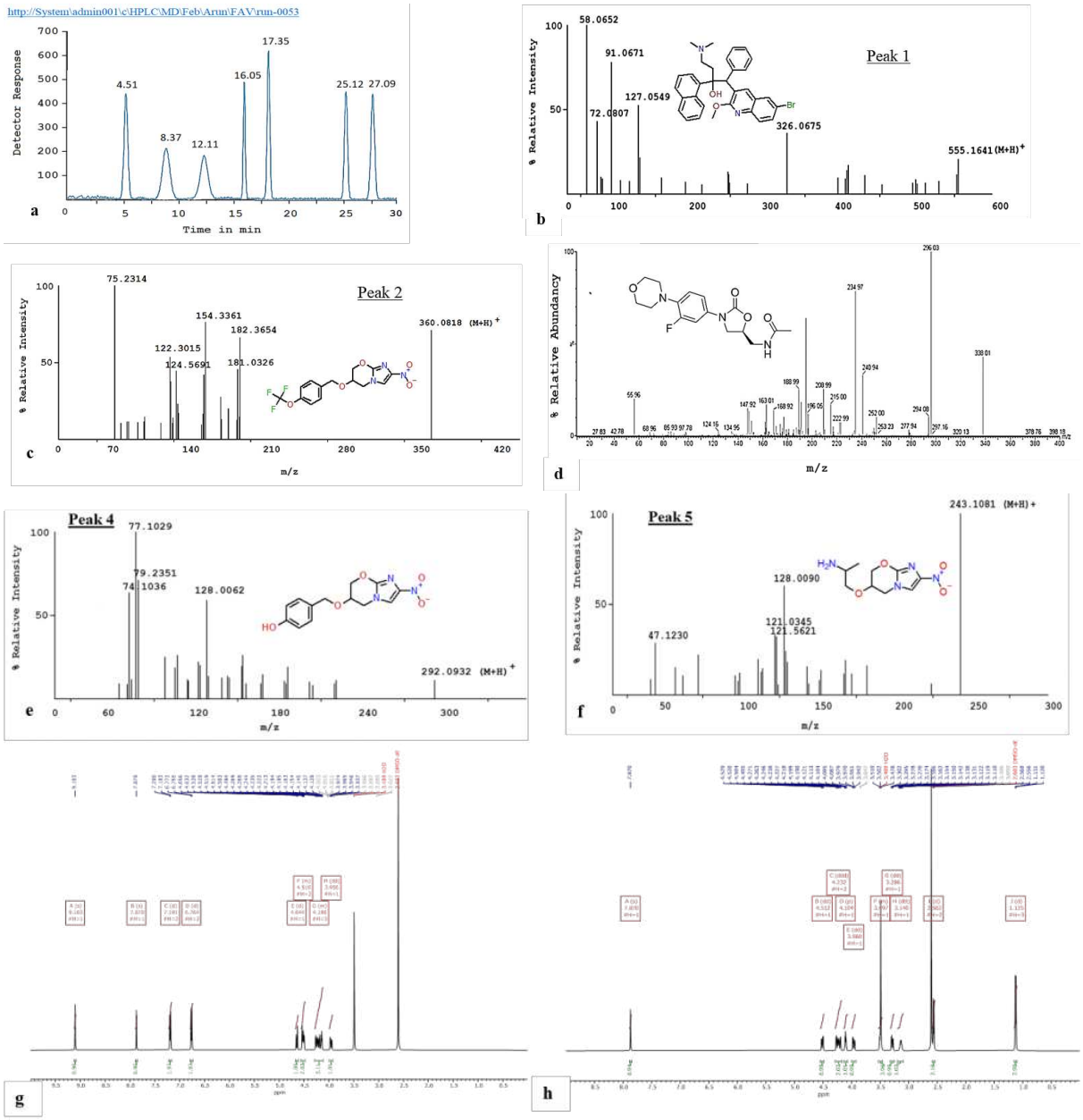



**Figure 3.** LC–MS/MS chromatographic, mass-spectrometric, and NMR characterization of the BPaL combination following acidic hydrolysis (0.1 N HCl, 80 °C for 3 h). **(A)** Chromatographic profile showing seven resolved peaks, including parent drug peaks at 4.51 min (BDQ), 8.37 min (PMD), and 12.11 min (LNZ), together with four additional degradation-associated peaks at 16.05, 17.35, 25.12, and 27.09 min. **(B–D)** Positive ion mass spectra of the parent drugs: (B) BDQ (m/z 555.1641), (C) PMD (m/z 360.0818), and (D) LNZ (m/z 338.01). **(E, F)** Mass spectra of two additional acid-associated components, showing precursor ions at m/z 292.0932 and 243.1081, respectively. **(G, H)** Corresponding NMR spectra for the structural characterization of the degradation-associated components of the samples. The proposed degradation product assignments remain tentative pending confirmation of their chromatographic peak correspondence and structural identity.

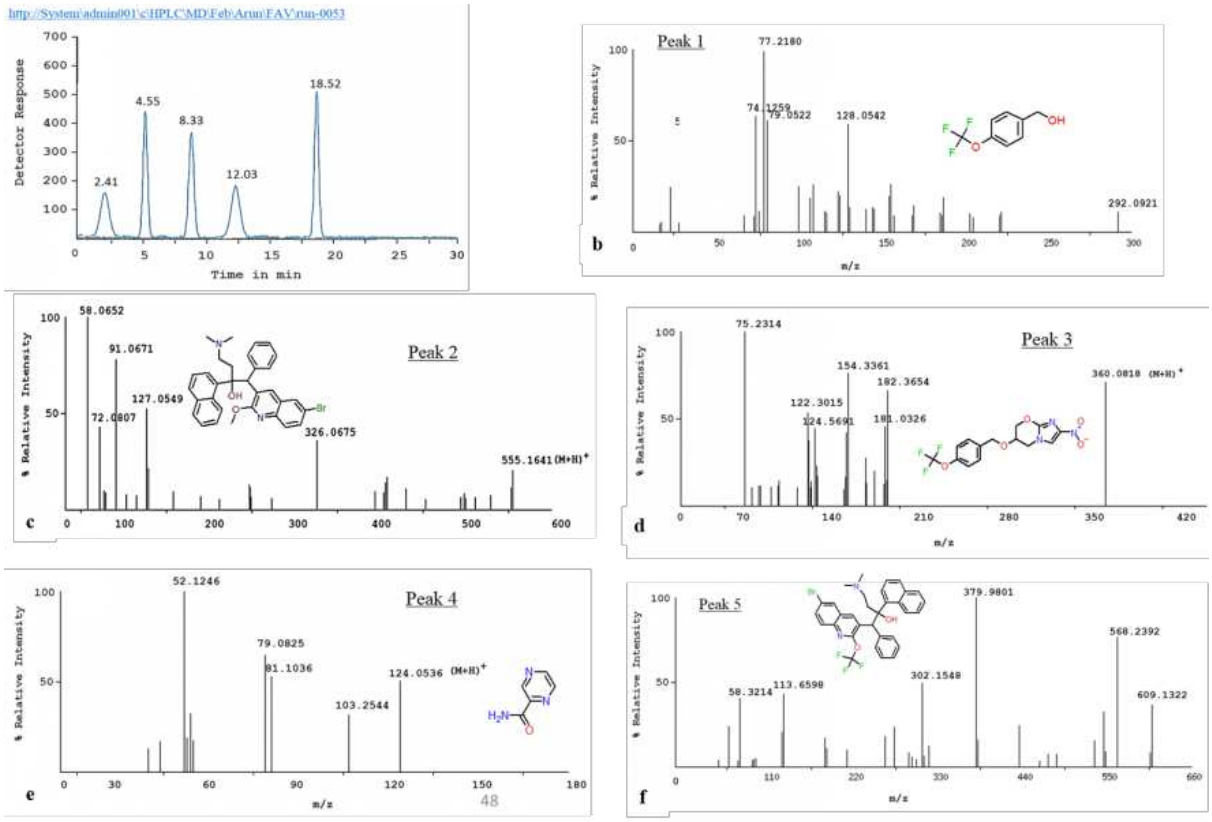
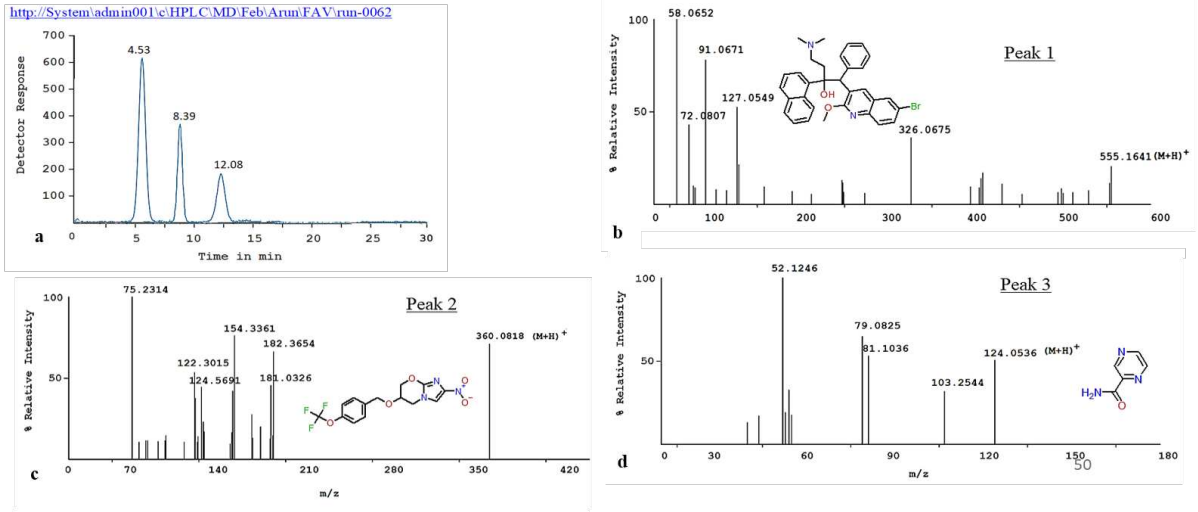



**Figure 4.** LC–MS/MS chromatographic and mass-spectrometric characterization of the BPaL combination following alkaline hydrolysis (0.1 N NaOH, 80 °C for 3 h). **(A)** Representative chromatogram showing five resolved peaks at retention times of 2.41, 4.55, 8.33, 12.03, and 18.52 min. **(B)** Mass spectrum of the degradation-associated component (peak 1), showing an ion at m/z 292.0921 and a prominent fragment at m/z 77.2180. **(C–E)** Mass spectra assigned to the parent drugs: (C) BDQ (peak 2; m/z 555.1641), (D) PMD (peak 3; m/z 360.0818), and (E) the component labeled as peak 4, provisionally assigned to LNZ. **(F)** Mass spectrum of the additional degradation-associated component (peak 5; retention time 18.52 min), displaying prominent ions at m/z 379.9801, 568.2392, and 609.1322. The structural assignments of the degradation-associated components and the identity of peak 4 require confirmation using original analytical data.



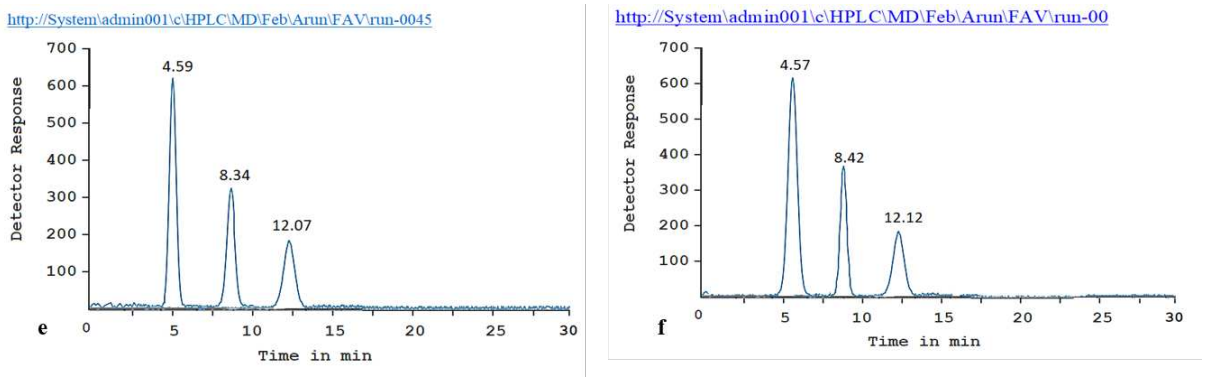



**Figure 5.** Comparative LC–MS/MS chromatographic and mass spectrometric profiles of the BPaL combination following neutral hydrolysis, thermal stress, and photolytic exposure. **(A)** Representative chromatogram obtained following neutral hydrolysis (water, 80 °C for 3 h), showing three parent-drug peaks at retention times of 4.53, 8.39, and 12.08 min, assigned to BDQ, PMD, and LNZ, respectively, respectively. **(B–D)** Corresponding mass spectra of the components assigned to (B) BDQ (m/z 555.1641), (C) PMD (m/z 360.0818), and (D) the third chromatographic peak, provisionally assigned to LNZ. **(E)** Chromatographic profile obtained following thermal stress (80 °C for 48 h), showing parent drug peaks at 4.59, 8.34, and 12.07 min. **(F)** Chromatographic profile obtained following photolytic exposure, showing parent drug peaks at 4.57, 8.42, and 12.12 min. No additional degradation-associated peaks were evident in the chromatograms under the investigated conditions.

**Table 3.** Comparative chromatographic findings following forced degradation of BDQ, PMD, and LNZ

| Stress condition | Additional peaks detected | Retention times of additional peaks (min) | Interpretation |
|---|---|---|---|
| Acidic hydrolysis | 4 | 16.05, 17.35, 25.12, 27.09 | Multiple potential degradation products detected |
| Alkaline hydrolysis | 2 | 2.41, 18.52 | Additional degradation-associated peaks detected |
| Neutral hydrolysis | 0 reported | — | No additional resolved peaks reported |
| Oxidative stress | Not established | — | Insufficient chromatographic evidence |
| Thermal stress | 0 reported | — | No additional resolved peaks reported |
| Photolytic stress | 0 reported | — | No additional resolved peaks reported |

### 3.5. LC–MS/MS Characterization of DPs

LC–MS/MS analysis of the stressed BPaL combination revealed additional chromatographic components under acidic and alkaline hydrolytic conditions, indicating the formation of potential DPs. Acidic hydrolysis generated four additional peaks at retention times of 16.05, 17.35, 25.12, and 27.09 min, whereas alkaline hydrolysis produced two additional peaks at 2.41 and 18.52 min (Figures 3A and 4A; Table 4). The mass spectrometric characteristics of the selected components were examined to investigate their possible structural relationships with the parent drug. Under acidic conditions, the mass spectra of the two degradation-associated components showed ions at m/z 292.0932 and 243.1081 (Figures 3E and 3F). The component with m/z 292.0932 exhibited prominent fragment ions at m/z 77.1029, 79.2351, 74.1036, and 128.0062, whereas the spectrum associated with m/z 243.1081 showed fragment ions at m/z 47.1230, 121.0345, 121.5621, and 128.0090. The accompanying NMR spectra provide supplementary structural information on the proposed acid-associated products (Figures 3G and 3H). However, the correspondence between these spectra and the individual chromatographic retention times requires verification; therefore, the proposed structures should be considered as tentative. Alkaline hydrolysis yielded an additional early-eluting component at 2.41 min, with a reported ion at m/z 292.0921 and characteristic spectral signals near m/z 77.2180 and 128.0542 (Figures 4A and 4B).

A second degradation-associated component appeared at 18.52 min and displayed prominent ions at m/z 379.9801, 568.2392, and 609.1322 (Figures 4A and 4F). These spectral differences indicate the presence of chemically distinct components in the alkaline-stressed sample. Nevertheless, the available data do not establish whether the observed ions represent protonated molecular species, fragment ions, adducts, or other ion forms in every case. The additional peaks observed under hydrolytic stress were chromatographically separated from the principal parent-drug peaks, supporting the utility of the developed method for detecting stress-associated changes. However, definitive assignment of individual DPs to BDQ, PMD, or LNZ requires confirmation through precursor-ion selection, product-ion relationships, and comparison with separately stressed parent-drug standards. Accurate-mass measurements and verified NMR assignments would further strengthen structural elucidation. Accordingly, the present findings support the detection and preliminary mass-spectrometric characterization of hydrolysis-associated products, while their chemical structures and degradation pathways remain provisional (Table 4).

Published BDQ impurity studies have illustrated the value

of complementary structural evidence. Vanavi and Rajput identified 11 DPs and one process-related impurity using ultraperformance liquid chromatography coupled with ESI mass spectrometry (UPLC/ESI–MS). They also isolated two major DPs for characterization using NMR, MS, and infrared spectroscopy [18]. Guo et al. used liquid chromatography–high-resolution tandem mass spectrometry (LC–HRMS/MS) and multistage MS for degradant assignment [16]. These approaches combine peak correspondence, fragmentation, and orthogonal characterization rather than equating an isolated ion signal with a confirmed structure. Schymanski et al. .

distinguished tentative candidates from confirmed structures supported by reference-standard MS, MS/MS, and retention-time matching [19]. This distinction is relevant here, although their framework was developed for high-resolution MS and does not establish that the present measurements are accurate-mass data. Reporting four decimal places alone does not demonstrate mass accuracy or resolving power. Any independently acquired accurate-mass measurements, including their source and calibration, must therefore be documented separately from API 4000 acquisition before elemental formulas or matches to published DPs can be asserted

**Table 4.** Chromatographic and mass-spectrometric characteristics of degradation-associated products detected following acidic and alkaline hydrolysis of the BPaL combination.

| Stress condition | DP designation | Retention time (min) | Reported ion (m/z) | Selected fragment ions (m/z) | Structural assignment |
|---|---|---|---|---|---|
| Acidic | A-DP1 | 16.05 | Not confirmed | — | Unassigned |
| Acidic | A-DP2 | 17.35 | Not confirmed | — | Unassigned |
| Acidic | A-DP3 | 25.12 | Not confirmed | — | Unassigned |
| Acidic | A-DP4 | 27.09 | Not confirmed | — | Unassigned |
| Acidic, spectral component 1 | A-MS1 | Retention-time correspondence unverified | 292.0932 | 77.1029, 79.2351, 74.1036, 128.0062 | Proposed PMD-related product; tentative |
| Acidic, spectral component 2 | A-MS2 | Retention-time correspondence unverified | 243.1081 | 47.1230, 121.0345, 121.5621, 128.0090 | Proposed PMD-related product; tentative |
| Alkaline | B-DP1 | 2.41 | 292.0921 | 77.2180, 128.0542 | Tentative; parent association unconfirmed |
| Alkaline | B-DP2 | 18.52 | Not established | 379.9801, 568.2392, 609.1322* | Tentative; parent association unconfirmed |

### 3.6. Proposed Degradation Pathways

The hydrolytic degradation pathways of PMD and BDQ were tentatively investigated by correlating the additional chromatographic peaks observed under acidic and alkaline conditions with their associated mass-spectrometric fragmentation patterns and proposed chemical structures. Acidic hydrolysis generated four additional chromatographic components, whereas alkaline hydrolysis produced two, indicating differences in the detectable transformation products formed under the investigated conditions (Figures 3 and 4; Table 4). The proposed degradation pathways are summarized schematically in Figure 6. For PMD, the acidic degradation-product spectra displayed ions at m/z 292.0932 and 243.1081, together with characteristic lower-mass signals, including m/z 77.1029, 128.0062, and 121.0345 (Figures 3E and 3F). The chemical structures depicted in the original spectra suggest possible modifications involving the substituted aromatic ether side chain and the nitroimidazooxazine-containing framework. Hydrolytic cleavage and subsequent structural rearrangements may therefore contribute to the formation of lower-molecular-mass products. However, these mechanisms remain hypothetical because the reported spectra do not independently establish the elemental compositions, bond-cleavage sites, or reaction sequence. The accompanying NMR spectra provide additional characterization data, although their correspondence with the individual chromatographic degradation peaks requires confirmation (Figures 3G and 3H).

Under alkaline conditions, an additional component eluting at 2.41 min displayed an ion at m/z 292.0921, with prominent signals at m/z 77.2180 and 128.0542 (Figure 4B). The structure proposed in the original figure contained a trifluoromethoxy-substituted aromatic moiety, suggesting a possible relationship with the aromatic ether region of PMD. Nevertheless, the proposed structure and reported molecular-ion assignment were not sufficiently consistent to establish a definitive hydrolytic product. Accordingly, this component is considered an unconfirmed PMD-related candidate rather than an identified degradation product. For BDQ, the parent compound exhibited a characteristic protonated ion at m/z 555.1641, with major fragmentation signals at m/z 58.0652, 91.0671, and 326.0675 (Figures 3B and 4C). These fragments provide a reference for evaluating possible structural changes in degradation-associated components. Under alkaline conditions, the additional component detected at 18.52 min exhibited prominent ions at m/z 379.9801, 568.2392, and 609.1322 (Figure 4F). Although the original investigation proposed a BDQ-related degradation structure, the relationship between these ions and the parent molecular ion requires further confirmation. Consequently, a specific BDQ hydrolytic cleavage mechanism cannot be established reliably from

the available spectral evidence. Collectively, the observed chromatographic and fragmentation patterns suggest that hydrolytic stress may affect different structural regions of PMD and BDQ, resulting in chemically distinct degradation-associated components. However, the proposed transformations should be interpreted cautiously because the available nominal-mass MS/MS data do not unequivocally establish molecular formulas or complete degradation pathways. Confirmation using accurate-mass spectrometry, verified NMR assignments, and independently stressed reference standards would be necessary to substantiate the proposed structures and reaction mechanisms (Figure 6).

The proposed pathways should be compared with published transformations, without implying that the products are identical. Nahata et al. described oxidation, hydrolysis, and rearrangement among the transformations associated with PMD degradation [14], whereas Guo et al. identified acid-induced BDQ demethylation and photolytic transformations involving tertiary alcohol and tertiary amine side-chain regions [16]. These observations establish plausible drug-specific transformations but do not confirm that the ions at m/z 292.0932, 243.1081, or 292.0921 represent their published products. Parent attribution also requires elemental consistency: BDQ contains bromine and a methoxy group but no fluorine or trifluoromethoxy substituents, whereas PMD contains a trifluoromethoxy-substituted aromatic ether [14,16]. Consequently, the candidates labeled as "trifluoromethoxy BDQ degradants" in the toxicity assessment cannot be justified as simple hydrolytic products of BDQ without additional evidence of their origins. Their labels, structures, and relationships with the separately stressed parent drugs require reconciliation before pathway or toxicity conclusions are assigned to BDQ. A name or similar nominal mass alone is insufficient to establish a correspondence with a published degradant [19].

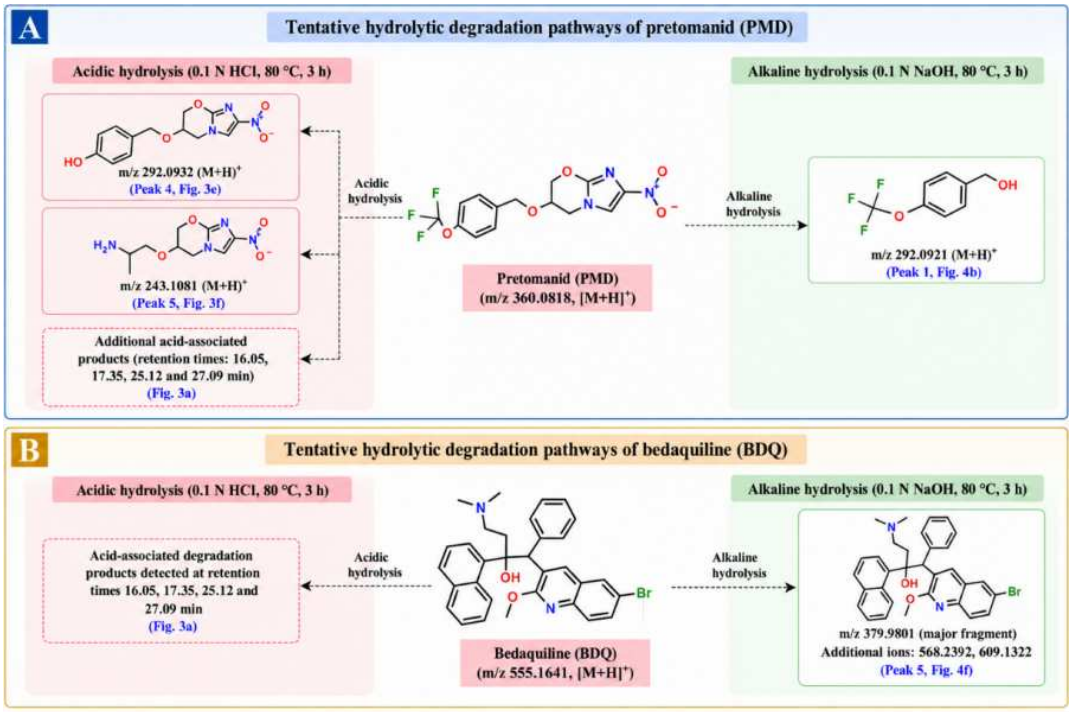



**Figure 6.** Proposed hydrolytic degradation pathways of (A) PMD and (B) BDQ under acidic (0.1 N HCl, 80 °C, 3 h) and alkaline (0.1 N NaOH, 80 °C, 3 h) conditions. **(A)** Tentative PMD-associated DPs displaying ions at m/z 292.0932 and 243.1081 under acidic conditions and m/z 292.0921 under alkaline conditions. **(B)** Proposed BDQ-associated degradation behavior, including an alkaline degradation-associated component exhibiting prominent ions at m/z 379.9801, 568.2392, and 609.1322. Dashed arrows indicate hypothetical transformation pathways inferred from chromatographic and mass spectrometric observations (Figures 3 and 4). The proposed structures and mechanisms remain tentative pending confirmation by accurate mass spectrometry and complementary structural characterization.

### 3.7. In silico Toxicity Assessment

ProTox-II was used to assess acute oral toxicity and select organ-specific and cellular endpoints for the proposed PMD- and BDQ-associated DPs. The predicted $LD_{50}$ values ranged from 350 to 550 mg/kg, placing all evaluated candidates in toxicity class IV (Table 5) [6]. Although the candidates shared an acute toxicity class, their predicted endpoint profiles were different. PMD-AH01 had the lowest predicted $LD_{50}$ (350 mg/kg) and positive hepatotoxicity, immunotoxicity, and cytotoxicity predictions. PMD-AH02 had a predicted $LD_{50}$ of 400 mg/kg, along with alerts for carcinogenicity and mutagenicity. Candidates provisionally labeled as BDQ-associated had predicted $LD_{50}$ values of 450–550 mg/kg. The candidate labeled "Trifluoromethoxy BDQ degradant" (500 mg/kg) had positive hepatotoxicity, carcinogenicity, immunotoxicity, and cytotoxicity predictions. Its labeled phenoxy derivative (450 mg/kg) exhibited immunotoxicity and cytotoxicity alerts, while the proposed [4-(trifluoromethoxy)phenyl] methanol candidate (550 mg/kg) exhibited a mutagenicity alert. The candidate labeled as "Trifluoromethoxy BDQ degradant

(alkaline)" (500 mg/kg) had positive hepatotoxicity and carcinogenicity predictions (Table 5). These labels are retained for correspondence with the submitted computational data, not as confirmation of the parent drug origin. The results suggest differences in the predicted toxicological profiles despite a shared acute toxicity class. However, these predictions depend on the submitted structures, and several DP identities and parent assignments remain unconfirmed. Therefore, the outputs represent preliminary computational assessments, not experimentally established hazards. Structural confirmation, reassessment using verified molecular representations, and appropriate experimental toxicological studies are required to establish their relevance to pharmaceutical stability and safety.

The computational results should be interpreted within the scope and limitations of structure-based toxicity prediction. ProTox-II uses separate models for acute toxicity, hepatotoxicity, carcinogenicity, mutagenicity, immunotoxicity, and cytotoxicity, with associated prediction confidence information [6]. Therefore, a shared acute oral toxicity class does not imply equivalent organ-specific or long-term toxicity. Nahata et al. combined PMD degradation profiling with in silico toxicity assessment [14], providing precedent for computational prioritization but not independent validation of the present candidate structures or $LD_{50}$ estimates. Guidance from the Organisation for Economic Co-operation and Development (OECD) on quantitative structure–activity relationship assessment emphasizes model validity, applicability to the target substance, and reliability of individual predictions [20]. Reproducible interpretation of the present outputs consequently requires verified structures or SMILES representations, the prediction-platform version, confidence information, and an applicability assessment where supported. The estimates of 350–550 mg/kg and endpoint alerts are predictions for the submitted structures, not measured toxicity values or literature-confirmed properties of the detected peaks. Structural uncertainty and inconsistent parent assignments must be resolved before impurity-specific safety conclusions can be drawn.

**Table 5.** Predicted acute oral toxicity and toxicological endpoints of proposed DPs using ProTox-II

| Proposed degradation product | Predicted $LD_{50}$ (mg/kg) | Toxicity class | Hepatotoxicity | Carcinogenicity | Immunotoxicity | Mutagenicity | Cytotoxicity |
|---|---|---|---|---|---|---|---|
| PMD-AH01 | 350 | IV | Yes | No | Yes | No | Yes |
| PMD-AH02 | 400 | IV | No | Yes | No | Yes | No |
| Trifluoromethoxy BDQ degradant | 500 | IV | Yes | Yes | Yes | No | Yes |
| Trifluoromethoxy phenoxy derivative of BDQ | 450 | IV | No | No | Yes | No | Yes |
| [4-(Trifluoromethoxy)phenyl]methanol | 550 | IV | No | No | No | Yes | No |
| Trifluoromethoxy BDQ degradant (alkaline) | 500 | IV | Yes | Yes | No | No | No |

## 4. Conclusion

An LC–MS/MS method intended for stability-indicating analysis was developed and evaluated for the simultaneous determination of BDQ, PMD, and LNZ. The three analytes eluted at 12.07 min within the 20-min analytical run, with reported precision of ≤1.85% RSD and recoveries of 98.54–101.82%. Acidic and alkaline hydrolysis produced additional degradation-associated peaks, whereas neutral, thermal, and photolytic stress produced no additional resolved peaks under the investigated conditions. Mass-spectrometric analysis supported the preliminary characterization of selected hydrolytic DPs. ProTox-II predictions placed the submitted candidate structures in acute oral toxicity class IV ($LD_{50}$: 350–550 mg/kg), with variable endpoint alerts. These findings support the method's potential for monitoring stress-induced changes in the BPaL combination. However, DP identities, quantitative degradation data, and outstanding validation parameters require verification before routine pharmaceutical quality control use. The study therefore provides a preliminary framework for integrated stability assessment and computational hazard evaluation of proposed BPaL-associated DPs.

**Ethics Approval And Consent To Participate**
Not applicable.

**Human And Animal Rights**
Not applicable.

**Consent For Publication**
Not applicable.

**Availability Of Data And Materials**
The datasets used and/or analyzed in this study are available from the corresponding author upon reasonable request.

**Funding**
This research did not receive any specific grants from any funding agency in the public, commercial, or not-for-profit sectors.

**Conflict Of Interest**
None of the authors have any competing financial interests or personal relationships that might have influenced their work.

**Acknowledgements**
The authors thank the School of Pharmacy, Anurag

University for providing technical facilities and support for conducting this research.

**References**


1. World Health Organization. Global tuberculosis report 2025. Geneva: World Health Organization; 2025. Available from: https://www.who.int/teams/global-programme-on-tuberculosis-and-lung-health/tb-reports/global-tuberculosis-report-2025
2. World Health Organization. WHO consolidated guidelines on tuberculosis: module 4—treatment and care. 2nd ed. Geneva: World Health Organization; 2026. ISBN: 978-92-4-012512-4. Available from: https://www.who.int/publications/i/item/9789240125124
3. Conradie F, Diacon AH, Ngubane N, et al. Treatment of highly drug-resistant pulmonary tuberculosis. N Engl J Med. 2020;382(10):893–902. doi: 10.1056/NEJMoa1901814.
4. International Council for Harmonisation of Technical Requirements for Pharmaceuticals for Human Use. ICH harmonised tripartite guideline Q1A(R2): stability testing of new drug substances and products. Geneva: ICH; 2003. Available from: https://www.ema.europa.eu/en/documents/scientific-guideline/ich-q-1-r2-stability-testing-new-drug-substances-and-products-step-5_en.pdf
5. International Council for Harmonisation of Technical Requirements for Pharmaceuticals for Human Use. ICH harmonised guideline Q2(R2): validation of analytical procedures. Geneva: ICH; 2024. Available from: https://www.fda.gov/regulatory-information/search-fda-guidance-documents/q2r2-validation-analytical-procedures
6. Banerjee P, Eckert AO, Schrey AK, Preissner R. ProTox-II: a webserver for the prediction of toxicity of chemicals. Nucleic Acids Res. 2018;46(W1):W257–W263. doi: 10.1093/nar/gky318.
7. International Council for Harmonisation of Technical Requirements for Pharmaceuticals for Human Use. ICH harmonised guideline Q14: analytical procedure development. Final version. Geneva: ICH; 2023.
8. Cheng W, Zhu H, Fu L, Zhang W, Zhang L, Lu Y. Development and application of an HPLC-MS/MS method for simultaneous determination of bedaquiline, pretomanid, and linezolid in plasma. Chin J Antituberc. 2025;47(5):613–622. doi: 10.19982/j.issn.1000-6621.20250004.
9. Blessy M, Patel RD, Prajapati PN, Agrawal YK. Development of forced degradation and stability indicating studies of drugs—A review. J Pharm Anal. 2014;4(3):159–165. doi: 10.1016/j.jpha.2013.09.003.
10. International Conference on Harmonisation of Technical Requirements for Registration of Pharmaceuticals for Human Use. ICH harmonised tripartite guideline Q1B: stability testing—photostability testing of new drug substances and products. Step 4 version. Geneva: ICH; 1996.
11. Singh S, Handa T, Narayanam M, Sahu A, Junwal M, Shah RP. A critical review on the use of modern sophisticated hyphenated tools in the characterization of impurities and degradation products. J Pharm Biomed Anal. 2012;69:148–173. doi: 10.1016/j.jpba.2012.03.044.
12. Weininger D. SMILES, a chemical language and information system. 1. Introduction to methodology and encoding rules. J Chem Inf Comput Sci. 1988;28(1):31–36. doi: 10.1021/ci00057a005.
13. Kim HY. Analysis of variance (ANOVA) comparing means of more than two groups. Restor Dent Endod. 2014;39(1):74–77. doi: 10.5395/rde.2014.39.1.74.
14. Nahata A, Joshi N, Patel M. Unveiling pretomanid profiling using LC–MS/MS: integrating in-silico toxicity assessment and molecular docking analysis. Chem Pap. 2025;79:817–837. doi: 10.1007/s11696-024-03818-3.
15. Sato Y, Takekuma Y, Daisho T, Kashiwagi H, Imai S, Sugawara M. Development of a method of liquid chromatography coupled with tandem mass spectrometry for simultaneous determination of linezolid and tedizolid in human plasma. Biol Pharm Bull. 2022;45(4):421–428. doi: 10.1248/bpb.b21-00798.
16. Guo K, Wang Y, Ma C. Characterization of stress degradation products of bedaquiline fumarate and bedaquiline by LC-PDA and LC-MS. J Pharm Biomed Anal. 2023;235:115658. doi: 10.1016/j.jpba.2023.115658.
17. Raju TS, Kutty OV, Ganesh V, Swamy PY. A validated stability-indicating LC method for the separation of enantiomer and potential impurities of linezolid using polar organic mode. J Pharm Anal. 2012;2(4):272–278. doi: 10.1016/j.jpha.2012.03.006.
18. Vanavi PJ, Rajput SJ. Separation and characterization of novel degradation and process related impurities of bedaquiline bulk drug. J Chromatogr Sci. 2022;60(7):678–691. doi: 10.1093/chromsci/bmab117.
19. Schymanski EL, Jeon J, Gulde R, Fenner K, Ruff M, Singer HP, Hollender J. Identifying small molecules via high resolution mass spectrometry: communicating confidence. Environ Sci Technol. 2014;48(4):2097–2098. doi: 10.1021/es5002105.
20. Organisation for Economic Co-operation and Development. (Q)SAR assessment framework: guidance for the regulatory assessment of (quantitative) structure–activity relationship models, predictions, and results based on multiple predictions. OECD Series on Testing and Assessment No. 386. Paris: OECD; 2023. Report No.: ENV/CBC/MONO(2023)32.